Egyptian Journal of Chemistry

http://ejchem.journals.ekb.eg/

Quinazolinone-Schiff's Base hybrids as Phosphodiesterase 4B inhibitors with dual activity against COPD and Lung Cancer

Mostafa A. Mansour[a*], Mohamed T. El-Saadi[b,c], Noha H. Amin[b], Joshua C. Canzoneri[d], Adam B. Keeton[d], Gary A. Piazza[d], Hamdy M. Abdel-Rahman[a,e]

[a] *Pharmaceutical Chemistry Department, Faculty of Pharmacy, Nahda University, 62764 Beni-Suef, Egypt.*

[b] *Medicinal Chemistry Department, Faculty of Pharmacy, Beni-Suef University, 62511 Beni-Suef, Egypt.*

[c] *Medicinal Chemistry Department, Faculty of Pharmacy, Sinai University, Ismailia, Egypt.*

[d] *USA Mitchell Cancer Institute Drug Discovery Laboratory, University of South Alabama, USA.*

[e] *Medicinal Chemistry Department, Faculty of Pharmacy, Assiut University, 71526 Assiut, Egypt.*

Abstract

A series of thirty compounds of quinazolinone-Schiff's base hybrids were rationally designed, synthesized, and evaluated for their in vitro Phosphodiesterase 4B inhibition, anti-lung and anti-colon cancer activities. Compounds **9, 16, 23, 29, 30, 31, 32** and **33**, each possessing a tri-hydroxy moiety, showed the highest inhibitory activity (56.05-89.07%) at 10 µM concentration if compared to rolipram. Compounds **16** and **23** showed good anti-lung cancer activity with IC_{50} 1.55 and 1.30 µM, respectively. Moreover, compound **16** showed high anti-colon cancer activity with IC_{50} 0.6 µM. Compound **33** showed good affinity and molecular binding modes towards the key amino acid Gln 443 and Phe 446 for inhibition of the target enzyme. Finally, active compounds showed good ADME calculations.

Keywords: Quinazolinone; Schiff's; Phosphodiesterase 4B; COPD; Lung; Colon; Cancer.

1. Introduction

Cancer is the second leading cause of death globally behind cardiovascular diseases and is responsible for an estimated 9.6 million deaths in 2018 [1]. At the same time, chronic obstructive pulmonary disease (COPD) affected about 65 million the global population in 2019, more than 3 million people death which corresponds to 5% of all deaths globally [2]. Interestingly, COPD has been found to be one of the major driving factors for lung cancer through increasing oxidative stress and resulting in DNA damage, chronic exposure to pro-inflammatory cytokines, repression of the DNA repair mechanisms and increased cellular proliferation[3]. Phosphodiesterases (PDEs), notably the PDE4 family, have played a critical role in maintaining the cellular levels of cyclic adenosine monophosphate (cAMP) and thus controlling major cellular inflammatory pathways. Accordingly, corresponding potential therapeutic uses of PDE4 inhibitors for different inflammatory disorders such as asthma and COPD have been of great interest [4]. Rolipram (**I**), a potent prototypic selective PDE4 inhibitor, has shown a great promise for the treatment of inflammation, chronic obstructive pulmonary disorders, cancers, and myocardium contractility disorder, but unfortunately dose-limiting side effects (nausea and emesis) and non-selectivity have limited its clinical development, (**Fig. 1**). Similarly,

*Corresponding author e-mail: mostafa.mansour@nub.edu.eg
Receive Date: 29 April 2020, Revise Date: 15 May 2020, Accept Date: 03 June 2020
DOI: 10.21608/EJCHEM.2020.28992.2624

Roflumilast (**II**) and Tofimilast (**III**) were discontinued from clinical development because of potential overlap of efficacy and undesired side effects, (Fig. 1) [4]. PDE4B inhibitors, which are believed to play a central role in inflammation, have yielded minimal undesirable side effects when compared to other PDE4 inhibitors [4,5]. In addition, PDE4 inhibitors may serve as potential targets for tumor cell growth inhibition and induction of apoptosis [6,7]. Accordingly, developing new selective PDE4B inhibitors with efficient anticancer activities has proven its therapeutic necessity and value [8].

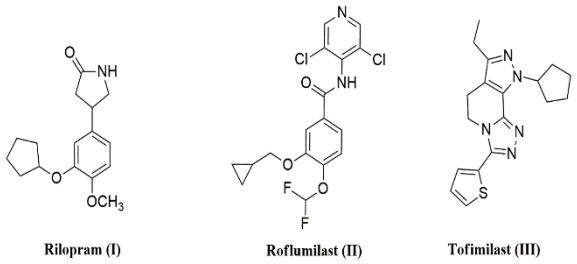

Figure 2: Chemical Structures of some Phosphodiesterase 4 inhibitors.

Xanthines (**IV**), nitraquazones (**V**) and *N*-acylhydrazones (NAH) (**VI**) have served as successful structural templates for selective PDE4 inhibitors; Specially Xanthines derivatives as Theophylline used as bronchodilator [9], yet novel templates are still needed to reach a selective and therapeutically safe treatment, (Fig. 2) [10.11].

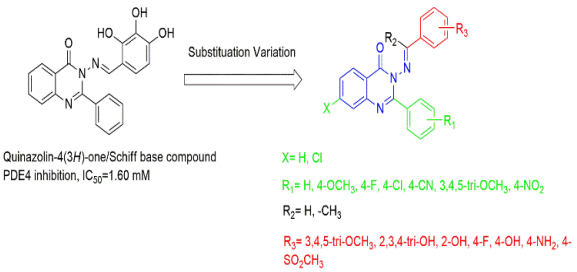

Figure 3: Lead modification optimization by substitution variation strategy.

After gathering previous research findings and as part of our ongoing research work to develop new and safe PDE inhibitors [5,12], the present work has dealt with structural merging of NAH (**VI**) scaffolds with quinazolines through molecular hybridization. Furthermore, lead optimization strategies were adopted through producing quinazoline-4-(3*H*)-ones/ Schiff bases with novel substituents and studying their possible selective PDE4 inhibitory activity, (**Fig. 3**).

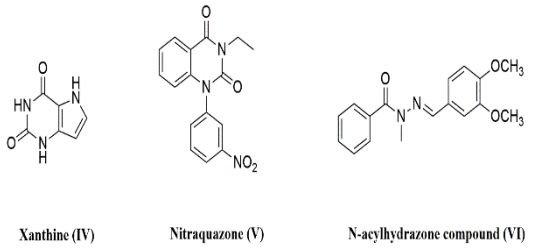

Figure 1: Chemical Structures of some structural templates for designing of PDE 4 inhibitors.

2. Experimental

2.1. Chemistry

Chemical reagents and solvents were obtained from Sigma Aldrich, Germany. Reactions were monitored by TLC: Pre-coated plastic sheets, 0.2 mm silica gel with fluorescent indicator (E. Merck). Melting points were determined on Stuart electrothermal melting point apparatus and were uncorrected. IR spectra were recorded as KBr disks on a Bruker spectrophotometer (Nahda University, Beni-Suef, Egypt). ^{1}H-NMR spectra were carried out on Bruker apparatus 400 MHz, (Beni-Suef University, Beni-Suef, Egypt) using TMS as internal reference, Chemical shifts (values are given in parts per million (ppm) using DMSO-d_6 (2.5) or $CDCl_3$ as solvents and coupling constants *(J)* in Hertz. Splitting patterns are designated as follows: s, singlet; d, doublet; t, triplet; q, quartet; dd, doublet of doublet; m, multiplet; bs, broad singlet. ^{13}C-NMR were recorded using Bruker 100 MHz NMR (Beni-Suef University, Beni-Suef, Egypt). Elemental analysis (C, H and N) were performed on VARIO-Elementer apparatus at (The Regional Center for Mycology and Biotechonology, Al-Azhar University, Egypt).

General method for synthesis of [(Un)Substituted 2-phenyl-4*H*-benzo[*d*][1,3]oxazin-4-one] compounds (2a-i):

Un/ substituted benzoyl chloride (0.1 mol) was added portion wise to a solution of un/ substituted anthranilic acid (0.05 mol) in pyridine (30 ml) with stirring in an ice bath (0-5 ºC) until solid mass formed or over the period of 30 minutes. The reaction

mixture was stirred at room temperature for another 30 minutes, neutralized with 20 % $NaHCO_3$ solution to pH = 7-8. The solid mass was filtered, washed many times with 20 % $NaHCO_3$ solution and distilled water until no odour of pyridine was detected, dried at oven (70-80ºC), and recrystallized from ethanol (96%) to give compounds **2a-i.**

2-Phenyl-4*H*-benzo[*d*][1,3]oxazin-4-one (2a):

Yield: 89 % as pale yellow powder, m.p.: 119-123 ºC, Reported 120 ºC [13].

2-(4-Methoxyphenyl)-4*H*-benzo[*d*][1,3]oxazin-4-one (2b):

White powder, M.wt. 253.25, yield: 95 %, m.p.: 153-154 °C; FT-IR (KBr) (υ_{max}/ cm^{-1}): 3057 (Ar-H), 2954 (aliphatic C-H), 1763 (C=O); ^{1}H-NMR ($CDCl_3$): (400 MHz) δ= 3.92 (s, 3H, OCH_3), 7.02 (d, *J*= 8.00 Hz, 2H, Ar-H), 7.50 (t, *J*= 8.00 Hz, 1H, Ar-H), 7.67 (d, *J*= 8.00 Hz, 1H, Ar-H), 7.82 (t, *J*= 8.00 Hz, 1H, Ar-H), 8.24 (d, *J*= 8.00 Hz, 1H, Ar-H), 8.29 (d, *J*= 8.00 Hz, 2H, Ar-H); Elemental analysis calculated for $C_{15}H_{11}NO_3$: C 71.14, H 4.38, N 5.53; Found C 71.29, H 4.40, N 5.61.

2-(4-Fluorophenyl)-4*H*-benzo[*d*][1,3]oxazin-4-one (2c):

White powder, M.wt. 241.22, yield: 85 %, m.p.: 170-173 °C; FT-IR (KBr) (υ_{max}/ cm^{-1}): 3040 (Ar-H), 1746 (C=O); ^{1}H-NMR ($CDCl_3$): (400 MHz) δ= 7.17-7.25 (m, 2H, Ar-H), 7.55 (t, *J*= 8.00 Hz, 1H, Ar-H), 7.71 (d, *J*= 8.00 Hz, 1H, Ar-H), 7.86 (t, *J*= 8.00 Hz, 1H, Ar-H), 8.27 (d, *J*= 8.00 Hz, 1H, Ar-H), 8.34-8.38 (m, 2H, Ar-H); Elemental analysis calculated for $C_{14}H_8FNO_2$: C 69.71, H 3.34, N 5.81; Found C 69.86, H 3.31, N 5.97.

2-(4-Chlorophenyl)-4*H*-benzo[*d*][1,3]oxazin-4-one (2d):

White powder, M.wt. 257.67, yield: 79 %, m.p.: 184-185 °C; FT-IR (KBr) (υ_{max}/ cm^{-1}): 3068 (Ar-H), 1755 (C=O), 1620 (C=C); ^{1}H-NMR ($CDCl_3$): (400 MHz) δ= 7.25-7.58 (m, 3H, Ar-H), 7.71 (d, *J*= 8.00 Hz, 1H, Ar-H), 7.86 (t, *J*= 8.00 Hz, 1H, Ar-H), 8.10 (d, *J*= 8.00 Hz, 1H, Ar-H), 8.26-8.30 (m, 2H, Ar-H); Elemental analysis calculated for $C_{14}H_8ClNO_2$: C 65.26, H 3.13, N 5.44; Found C 65.38, H 3.15, N 5.49.

7-Chloro-2-(4-methoxyphenyl)-4*H*-benzo[*d*][1,3]oxazin-4-one (2e):

White powder, M.wt. 287.70, yield: 80 %, m.p.: 290-292 °C; FT-IR (KBr) (υ_{max}/ cm^{-1}): 3063 (Ar-H), 1760 (C=O), 1617 (C=C); ^{1}H-NMR (DMSO-d_6): (400 MHz) δ= 3.85 (s, 3H, OCH_3), 7.16 (d, *J*= 8.00 Hz, 2H, Ar-H), 7.62 (d, *J*= 8.00 Hz, 1H, Ar-H), 7.76 (s, 1H, Ar-H), 8.15 (d, *J*= 8.00 Hz, 2H, Ar-H), 8.58 (s, 1H, Ar-H); Elemental analysis calculated for $C_{15}H_{10}ClNO_3$: C 62.62, H 3.50, N 4.87; Found C 62.89, H 3.67, N 4.65.

4-(4-Oxo-4*H*-benzo[*d*][1,3]oxazin-2-yl)benzonitrile (2f):

White powder, M.wt. 248.24, yield: 65 %, m.p.: 187-189 °C; FT-IR (KBr) (υ_{max}/ cm^{-1}): 3075 (Ar-H), 2231 (C≡N), 1762 (C=O), 1623 (C=C); ^{1}H-NMR (DMSO-d_6): (400 MHz) δ= 7.60 (t, *J*= 8.00 Hz, 1H, Ar-H), 7.63 (d, *J*= 8.00 Hz, 2H, Ar-H), 7.73 (s, 1H, Ar-H), 7.95 (t, *J*= 8.00 Hz, 1H, Ar-H), 8.15 (d, *J*= 8.00 Hz, 1H, Ar-H), 8.19 (d, *J*= 8.00 Hz, 2H, Ar-H); Elemental analysis calculated for $C_{15}H_8N_2O_2$: C 72.58, H 3.25, N 11.28; Found C 72.84, H 3.08, N 11.49.

2-(3,4,5-Trimethoxyphenyl)-4*H*-benzo[*d*][1,3]oxazin-4-one (2g):

White powder, M.wt. 313.30, yield: 93 %, m.p.: 207-209 °C; FT-IR (KBr) (υ_{max}/ cm^{-1}): 3003 (Ar-H), 2986 (aliphatic C-H), 1756 (C=O), 1616 (C=C); ^{1}H-NMR (DMSO-d_6): (400 MHz) δ= 3.88 (s, 3H, OCH_3), 3.91 (s, 6H, OCH_3), 7.46 (s, 2H, Ar-H), 7.62 (t, *J*= 8.00 Hz, 1H, Ar-H), 7.73 (d, *J*= 8.00 Hz, 1H, Ar-H), 7.95 (t, *J*= 8.00 Hz, 1H, Ar-H), 8.16 (d, *J*= 8.00 Hz, 1H, Ar-H); Elemental analysis calculated for $C_{17}H_{15}NO_5$: C 65.17, H 4.83, N 4.47; Found C 65.39, H 4.98, N 4.60.

2-(4-Nitrophenyl)-4*H*-benzo[*d*][1,3]oxazin-4-one (2h):

Yellowish white powder, M.wt. 268.22, yield: 73 %, m.p.: 179-182 °C; FT-IR (KBr) (υ_{max}/ cm^{-1}): 3069 (Ar-H), 1763 (C=O), 1622 (C=C); ^{1}H-NMR (DMSO-d_6): (400 MHz) δ= 7.63 (t, *J*= 8.00 Hz, 1H, Ar-H), 7.72 (d, *J*= 8.00 Hz, 2H, Ar-H), 7.95 (t, *J*= 8.00 Hz, 1H, Ar-H), 8.16 (d, *J*= 8.00 Hz, 2H, Ar-H), 8.25 (t, *J*= 8.00 Hz, 2H, Ar-H); Elemental analysis calculated for $C_{14}H_8N_2O_4$: C 62.69, H 3.01, N 10.44; Found C 62.53, H 3.14, N 10.28.

7-Chloro-2-(4-fluorophenyl)-4*H*-benzo[*d*][1,3]oxazin-4-one (2i):

White powder, M.wt. 275.66, yield: 64 %, m.p.: 220-224 °C; FT-IR (KBr) (υ_{max}/ cm^{-1}): 3088 (Ar-H), 1779 (C=O), 1622 (C=C); ^{1}H-NMR (DMSO-d_6): (400 MHz) δ= 7.43-7.48 (m, 2H, Ar-H), 7.94-8.04 (m, 2H, Ar-H), 8.14 (d, *J*= 8.00 Hz, 2H, Ar-H), 8.65 (s, 1H, Ar-H); Elemental analysis calculated for $C_{14}H_7ClFNO_2$: C 61.00, H 2.56, N 5.08; Found C 60.86, H 2.49, N 5.34.

General method for synthesis of 3-Amino-2-(un)substituted phenylquinazolin-4(3*H*)-one compounds (3a-i):

A mixture of compounds **2a-i** (0.1 mol) and hydrazine mono hydrate 40% (0.1 mol, 12.5 ml) was refluxed in ethanol for 4 hours. The reaction was monitored with TLC (system 7:3 petroleum ether: ethyl acetate), then poured on crushed ice, filtered and washed many times with distilled water, dried at oven (70-80ºC), recrystallized from ethanol (96%) to give a fragile solid mass.

3-Amino-2-phenylquinazolin-4(3*H*)-one (3a):

Yield: 44 % as white fluffy solid, m.p.: 185-187 ºC, Reported 196 ºC [13].

3-Amino-2-(4-methoxyphenyl)quinazolin-4(3*H*)-one (3b):

Brownish white fluffy solid mass, M.wt. 267.28, yield: 80 %, m.p.: 175-177 °C; FT-IR (KBr) (υ_{max}/ cm^{-1}): 3427,3340 (NH_2), 3047 (Ar-H), 1664 (C=O); ^{1}H-NMR ($CDCl_3$): (400 MHz) δ= 3.89 (s, 3H, OCH_3), 5.24 (s, 2H, NH_2, D_2O exchangeable), 6.97 (d, *J*= 8.00 Hz, 2H, Ar-H), 7.53 (t, *J*= 8.00 Hz, 1H, Ar-H), 7.78 (t, *J*= 8.00 Hz, 1H, Ar-H), 7.91 (d, *J*= 8.00 Hz, 2H, Ar-H), 7.96-7.99 (m, 1H, Ar-H), 8.29 (d, *J*= 8.00 Hz, 1H, Ar-H); Elemental analysis calculated for $C_{15}H_{13}N_3O_2$: C 67.40, H 4.90, N 15.72; Found C 67.63, H 4.98, N 15.87.

3-Amino-2-(4-fluorophenyl)quinazolin-4(3*H*)-one (3c):

Yellowish white fluffy solid mass, M.wt. 255.25, yield: 78 %, m.p.: 200-203 °C; FT-IR (KBr) (υ_{max}/ cm_{-1}): 3491,3387 (NH_2), 3007 (Ar-H), 1668 (C=O); ^{1}H-NMR ($CDCl_3$): (400 MHz) δ= 5.53 (s, 2H, NH_2, D_2O exchangeable), 7.20-7.24 (m, 3H, Ar-H), 7.48-7.55 (m, 3H, Ar-H), 8.57 (d, *J*= 8.00 Hz, 2H, Ar-H); Elemental analysis calculated for $C_{14}H_{10}FN_3O$: C 65.88, H 3.95, N 16.46; Found C 66.01, H 4.01, N 16.72.

3-Amino-2-(4-chlorophenyl)quinazolin-4(3*H*)-one (3d):

White fluffy solid mass, M.wt. 271.70, yield: 71 %, m.p.: 205-210 °C; FT-IR (KBr) (υ_{max}/ cm^{-1}): 3425,3340 (NH_2), 3007 (Ar-H), 1667 (C=O); ^{1}H-NMR ($CDCl_3$): (400 MHz) δ= 5.73 (s, 2H, NH_2, D_2O exchangeable), 7.15-7.48 (m, 3H, Ar-H), 7.52-7.56 (m, 3H, Ar-H), 8.57 (d, *J*= 8.00 Hz, 2H, Ar-H); Elemental analysis calculated for $C_{14}H_{10}ClN_3O$: C 61.89, H 3.71, N 15.47; Found C 62.04, H 3.79, N 15.59.

3-Amino-7-chloro-2-(4-methoxyphenyl)quinazolin-4(3*H*)-one (3e):

White fluffy solid mass, M.wt. 301.73, yield: 88 %, m.p.: 191 °C; FT-IR (KBr) (υ_{max}/ cm^{-1}): 3441,3421 (NH_2), 3089 (Ar-H), 2923 (Aliphatic C-H), 1667 (C=O); ^{1}H-NMR (DMSO-d_6): (400 MHz) δ= 3.86 (s, 3H, OCH_3), 5.71 (s, 2H, NH_2, D_2O exchangeable), 7.13 (d, *J*= 8.00 Hz, 2H, Ar-H), 7.76-7.94 (m, 2H, Ar-H), 8.16 (d, *J*= 8.00 Hz, 2H, Ar-H), 8.77 (s, 1H, Ar-H); Elemental analysis calculated for $C_{15}H_{12}ClN_3O_2$: C 59.71, H 4.01, N 13.93; Found C 59.94, H 4.23, N 14.21.

4-(3-Amino-4-oxo-3,4-dihydroquinazolin-2-yl)benzonitrile (3f):

Off-white fluffy solid mass, M.wt. 262.27, yield: 62 %, m.p.: 220 °C; FT-IR (KBr) (υ_{max}/ cm^{-1}): 3317,3308 (NH_2), 2233 (C≡N), 1668 (C=O); ^{1}H-NMR (DMSO-d_6): (400 MHz) δ= 5.71 (s, 2H, NH_2, D_2O exchangeable), 7.57 (t, *J*= 8.00 Hz, 1H, Ar-H), 7.72 (d, *J*= 8.00 Hz, 2H, Ar-H), 7.85 (t, *J*= 8.00 Hz, 1H, Ar-H), 8.19 (d, *J*= 8.00 Hz, 2H, Ar-H), 8.59 (d, *J*= 8.00 Hz, 2H, Ar-H); Elemental analysis calculated for $C_{15}H_{10}N_4O$: C 68.69, H 3.84, N 21.36; Found C 68.52, H 3.98, N 21.62.

3-Amino-2-(3,4,5-trimethoxyphenyl)quinazolin-4(3*H*)-one (3g):

White powder, M.wt. 327.33, yield: 82 %, m.p.: 193-195 °C; FT-IR (KBr) (υ_{max}/ cm^{-1}): 3334,3322 (NH_2), 3063 (Ar-H), 2991 (Aliphatic C-H), 1661 (C=O); ^{1}H-NMR (DMSO-d_6): (400 MHz) δ= 3.74 (s, 3H, OCH_3), 3.82 (s, 6H, OCH_3), 5.71 (s, 2H, NH_2, D_2O exchangeable), 7.11 (s, 2H, Ar-H), 7.57 (t, *J*= 8.00 Hz, 1H, Ar-H), 7.83 (t, *J*= 8.00 Hz, 1H, Ar-H), 8.19 (d, *J*= 8.00 Hz, 1H, Ar-H), 8.62 (d, *J*= 8.00 Hz, 1H, Ar-H); Elemental analysis calculated for $C_{17}H_{17}N_3O_4$: C 62.38, H 5.23, N 12.84; Found C 62.63, H 5.11, N 13.08.

3-Amino-2-(4-nitrophenyl)quinazolin-4(3*H*)-one (3h):

White powder, M.wt. 282.25, yield: 76 %, m.p.: 186-187 °C; FT-IR (KBr) (υ_{max}/ cm^{-1}): 3317,3301 (NH_2), 3054 (Ar-H), 1667 (C=O); ^{1}H-NMR (DMSO-d_6): (400 MHz) δ= 5.67 (s, 2H, NH_2, D_2O exchangeable), 7.18 (t, *J*= 8.00 Hz, 1H, Ar-H), 7.32 (t, *J*= 8.00 Hz, 1H, Ar-H), 7.56 (t, *J*= 8.00 Hz, 1H, Ar-H), 7.79 (d, *J*= 8.00 Hz, 2H, Ar-H), 8.00 (t, *J*= 8.00 Hz, 1H, Ar-H), 8.62 (d, *J*= 8.00 Hz, 2H, Ar-H); Elemental analysis calculated for $C_{14}H_{10}N_4O_3$: C 59.57, H 3.57, N 19.85; Found C 59.84, H 3.69, N 20.11.

3-Amino-7-chloro-2-(4-fluorophenyl)quinazolin-4(3*H*)-one (3i):

White powder, M.wt. 289.69, yield: 79 %, m.p.: 227-229 °C; FT-IR (KBr) (υ_{max}/ cm^{-1}): 3375,3331 (NH_2), 3090 (Ar-H), 1672 (C=O); ^{1}H-NMR (DMSO-d_6): (400 MHz) δ= 5.68 (s, 2H, NH_2, D_2O exchangeable), 7.55 (d, *J*= 8.00 Hz, 2H, Ar-H), 7.88-8.02 (m, 2H, Ar-H), 8.15 (d, *J*= 8.00 Hz, 2H, Ar-H), 8.72 (s, 1H, Ar-H); Elemental analysis calculated for $C_{14}H_9ClFN_3O$: C 58.04, H 3.13, N 14.51; Found C 58.21, H 3.28, N 14.79.

General method for synthesis of the final compounds (4-33):

A mixture of compounds **3a-i** (0.001 mol) and appropriate aldehyde or acetophenone (0.001 mol) was refluxed in absolute ethanol in presence of 5 drops of glacial acetic acid to 4-10 hours. The reaction was monitored with TLC (system 6:4 petroleum ether: ethyl acetate) till completion. Then the solution was cooled and the solid mass precipitated, filtered off and washed with distilled water, dried and recrystallized from ethanol.

2-Phenyl-3-((3,4,5-trimethoxybenzylidene)amino)quinazolin-4(3*H*)-one (4):

White powder, M.wt. 415.44, Yield: 90 %, m.p.: 194-198 °C; FT-IR (KBr) (υ_{max}/ cm^{-1}): 3020 (Ar-H), 2934 (aliphatic CH), 1686 (C=O), 1608; ^{1}H-NMR ($CDCl_3$): (400 MHz) δ= 3.84 (s, 6H, OCH_3), 3.92 (s, 3H, OCH_3), 6.93 (s, 2H, Ar-H), 7.49 (t, *J*= 8.00 Hz, 1H, Ar-H), 7.58 (t, *J*= 8.00 Hz, 2H, Ar-H), 7.77 (d, *J*= 8.00 Hz, 2H, Ar-H), 7.82-7.94 (m, 2H, Ar-H), 9.1 (s, 1H, N=C*H*); Elemental analysis calculated for $C_{24}H_{21}N_3O_4$: C 69.39, H 5.10, N 10.11; Found C 69.53, H 5.18, N 10.34.

3-((4-Fluorobenzylidene)amino)-2-phenylquinazolin-4(3*H*)-one (5):

Yellow powder, M.wt. 343.35, Yield: 91 %, m.p.: 153-157 °C; FT-IR (KBr) (υ_{max}/ cm^{-1}): 3003 (Ar-H), 1684 (C=O), 1616; ^{1}H-NMR ($CDCl_3$): (400 MHz) δ= 7.11-8.39 (m, 13H, Ar-H), 9.06 (s, 1H, N=C*H*) ; Elemental analysis calculated for $C_{21}H_{14}FN_3O$: C 73.46, H 4.11, N 12.24; Found C 73.61, H 4.16, N 12.47.

3-((1-(4-Aminophenyl)ethylidene)amino)-2-phenylquinazolin-4(3*H*)-one (6):

Yellow powder, M.wt. 354.40, Yield: 61 %, m.p.: 187-190 °C; FT-IR (KBr) (υ_{max}/ cm^{-1}): 3457, 3333 (NH_2), 1688 (C=O); ^{1}H-NMR ($CDCl_3$): (400 MHz) δ= 1.90 (s, 3H, aliphatic CH_3), 5.11 (s, 2H, NH_2, D_2O exchangeable), 7.53-7.59 (m, 5H, Ar-H), 7.80-7.85 (m, 4H, Ar-H), 7.94 (d, *J*= 8.00 Hz, 2H, Ar-H), 8.33 (d, *J*= 8.00 Hz, 2H, Ar-H); Elemental analysis calculated for $C_{22}H_{18}N_4O$: C 74.56, H 5.12, N 15.81; Found C 74.72, H 5.18, N 16.04.

3-((1-(4-(Methylsulfonyl)phenyl)ethylidene)amino)-2-phenylquinazolin-4(3*H*)-one (7):

Yellowish white powder, M.wt. 417.11, Yield: 82.5 %, m.p.: 200-201 °C; FT-IR (KBr) (υ_{max}/ cm^{-1}): 3030 (Ar-H), 2923 (Aliphatic C-H), 1665 (C=O), 1316 (S=O); ^{1}H-NMR (DMSO-d_6): (400 MHz) δ= 1.99 (s, 3H, aliphatic CH_3), 2.51 (s, 3H, -SO_2-C$\underline{H_3}$), 7.45 (d, *J*= 8.00 Hz, 2H, Ar-H), 7.57 (t, *J*= 8.00 Hz, 2H, Ar-H), 7.72 (d, *J*= 8.00 Hz, 2H, Ar-H), 7.80-7.87 (m, 5H, Ar-H), 8.21 (d, *J*= 8.00 Hz, 2H, Ar-H); Elemental analysis calculated for $C_{22}H_{17}ClN_4O$: C 66.17, H 4.59, N 10.07; Found C 66.44, H 4.62, N 10.42.

2-(4-Methoxyphenyl)-3-((3,4,5-trimethoxybenzylidene)amino)quinazolin-4(3*H*)-one (8):

Yellowish white powder, M.wt. 445.47, Yield: 93 %, m.p.: 193-196 °C; FT-IR (KBr) (υ_{max}/ cm^{-1}): 3067 (Ar-H), 2966 (Aliphatic C-H), 1667 (C=O), 1647, 1605; ^{1}H-NMR ($CDCl_3$): (400 MHz) δ=3.90 (s, 3H, OCH_3), 3.96 (s, 6H, OCH_3), 3.97 (s, 3H, OCH_3), 6.90 (s, 2H, Ar-H), 7.00 (d, *J*= 8.00 Hz, 2H, Ar-H), 7.05 (d, *J*= 8.00 Hz, 2H, Ar-H), 7.83 (t, *J*= 8.00 Hz, 2H, Ar-H), 7.89 (d, *J*= 8.00 Hz, 1H, Ar-H), 8.32 (d, *J*= 8.00 Hz, 1H, Ar-H), 9.09 (ds, 1H, N=C*H*); Elemental analysis calculated for $C_{25}H_{23}N_3O_5$: C 67.41, H 5.20, N 9.43; Found C 67.43, H 5.29, N 9.61.

2-(4-Methoxyphenyl)-3-((2,3,4-trihydroxybenzylidene)amino)quinazolin-4(3*H*)-one (9):

Yellowish white crystals, M.wt. 403.39, Yield: 53.8 %, m.p.: 250-259 °C; FT-IR (KBr) (υ_{max}/ cm^{-1}): 3382 (broad, OH), 3007 (Ar-H), 2926 (Aliphatic C-H), 1633 (C=O) 1602 (C=C); ^{1}H-NMR (DMSO-d_6): (400 MHz) δ=3.86 (s, 3H, OCH_3), 6.41 (d, *J*=8.00 Hz, 1H, Ar-H), 6.84 (d, *J*=8.00 Hz, 1H, Ar-H), 7.14 (d, *J*=8.00 Hz, 2H, Ar-H), 7.26 (t, *J*=8.00 Hz, 1H, Ar-H), 7.62 (t, *J*=8.00 Hz, 1H, Ar-H), 7.90-7.94 (m, 3H, Ar-H), 8.60 (d, *J*=8.00 Hz, 1H, Ar-H), 9.56 (s, 1H, N=C*H*), 11.40 (s, 1H, phenolic OH, D_2O exchangeable), 11.94 (s, 1H, phenolic OH, D_2O

exchangeable), 12.21 (s, 1H, phenolic OH, D_2O exchangeable); ^{13}C-NMR (DMSO-d_6): (100 MHz) δ=55.98, 108.24, 111.28, 114.69, 120.04, 121.29, 121.65, 123.29, 127.00, 128.92, 129.41, 133.16, 133.21, 140.16, 148.11, 149.49, 151.56, 162.77, 164.53, 164.93; Elemental analysis calculated for $C_{22}H_{17}N_3O_5$: C 65.50, H 4.25, N 10.42; Found C 65.72, H 4.32, N 10.65.

3-((2-Hydroxybenzylidene)amino)-2-(4-methoxyphenyl)quinazolin-4(3*H*)-one (10):

White powder, M.wt. 371.39, Yield: 61.1 %, m.p.: 228-231 °C; FT-IR (KBr) (υ_{max}/ cm^{-1}): 3297 (broad, OH), 3004 (Ar-H), 2981 (Aliphatic C-H), 1687 (C=O); ^{1}H-NMR ($CDCl_3$): (400 MHz) δ= 3.86 (s, 3H, OCH_3), 6.99-7.03 (m, 4H, Ar-H), 7.40-7.46 (m, 2H, Ar-H), 7.58 (t, *J*= 8.00 Hz, 1H, Ar-H), 7.67 (d, *J*= 8.00 Hz, 2H, Ar-H), 7.84 (t, *J*= 8.00 Hz, 1H, Ar-H), 8.01 (d, *J*= 8.00 Hz, 1H, Ar-H), 8.37 (d, *J*= 8.00 Hz, 1H, Ar-H), 9.15 (s, 1H, N=C*H*), 10.14 (s, 1H, phenolic OH, D_2O exchangeable); Elemental analysis calculated for $C_{22}H_{17}N_3O_3$: C 71.15, H 4.61, N 11.31; Found C 71.32, H 4.65, N 11.47.

3-((4-Fluorobenzylidene)amino)-2-(4-methoxyphenyl)quinazolin-4(3*H*)-one (11):

White powder, M.wt. 373.38, Yield: 80.5 %, m.p.: 241-243 °C; FT-IR (KBr) (υ_{max}/ cm^{-1}): 3010 (Ar-H), 1684 (C=O); ^{1}H-NMR ($CDCl_3$): (400 MHz) δ= 3.91 (s, 3H, OCH_3), 7.04 (d, *J*=8.00 Hz, 4H, Ar-H), 7.15 (t, *J*= 8.00 Hz, 2H, Ar-H), 7.24 (t, *J*= 8.00 Hz, 2H, Ar-H), 7.88-7.99 (m, 2H, Ar-H), 8.04 (d, J=8.00 Hz, 2H, Ar-H), 8.58 (s, 1H, N=C*H*); Elemental analysis calculated for $C_{22}H_{16}FN_3O_2$: C 70.77, H 4.32, N 11.25; Found C 70.89, H 4.36, N 11.38.

3-((4-Hydroxybenzylidene)amino)-2-(4-methoxyphenyl)quinazolin-4(3*H*)-one (12):

Dark brown powder, M.wt. 371.39, Yield: 72.2 %, m.p.: 252-255 °C; FT-IR (KBr) (υ_{max}/ cm^{-1}): 3329 (broad, OH), 3061 (Ar-H), 1663 (C=O); ^{1}H-NMR ($CDCl_3$): (400 MHz) δ= 3.38 (s, 3H, OCH_3), 7.22-7.53 (m, 4H, Ar-H), 7.55-7.67 (m, 3H, Ar-H), 7.72 (t, *J*= 8.00 Hz, 1H, Ar-H), 7.82 (d, *J*= 8.00 Hz, 2H, Ar-H), 8.13 (d, *J*= 8.00 Hz, 2H, Ar-H), 9.79 (s, 1H, N=C*H*), 10.52 (s, 1H, phenolic OH, D_2O exchangeable); Elemental analysis calculated for $C_{22}H_{17}N_3O_3$: C 73.89, H 4.43, N 12.31; Found C 71.34, H 4.68, N 11.48.

3-((1-(4-Aminophenyl)ethylidene)amino)-2-(4-methoxyphenyl)quinazolin-4(3*H*)-one (13):

White powder, M.wt. 384.43, Yield: 72.9 %, m.p.: 190-191 °C; FT-IR (KBr) (υ_{max}/ cm^{-1}): 3398, 3329 (NH_2), 3007 (Ar-H), 1681 (C=O); ^{1}H-NMR ($CDCl_3$): (400 MHz) δ= 1.68 (s, 3H, aliphatic CH_3), 3.87 (s, 3H, OCH_3), 5.53 (s, 2H, NH_2, D_2O exchangeable), 7.07 (d, *J*= 8.00 Hz, 2H, Ar-H), 7.81-7.86 (m, 2H, Ar-H), 7.94-8.09 (m, 2H, Ar-H), 8.26 (d, *J*= 8.00 Hz, 2H, Ar-H), 8.33-8.43 (m, 2H, Ar-H); Elemental analysis calculated for $C_{23}H_{20}N_4O_2$: C 71.86, H 5.24, N 14.57; Found C 72.04, H 5.31, N 14.78.

2-(4-Methoxyphenyl)-3-((1-(4(methylsulfonyl)phenyl)ethylidene)amino)quinazolin-4(3*H*)-one (14):

Yellowish white powder, M.wt. 447.51, Yield: 81.39 %, m.p.: 189-191 °C; FT-IR (KBr) (υ_{max}/ cm^{-1}): 3013 (Ar-H), 2968 (Aliphatic C-H), 1672 (C=O); ^{1}H-NMR (DMSO-d_6): (400 MHz) δ= 1.99 (s, 3H, aliphatic CH_3), 2.48 (s, 3H, -SO_2-C<u>H</u>$_3$), 3.85 (s, 3H, OCH_3), 7.44 (d, *J*=8.00, 2H, Ar-H), 7.48 (d, *J*= 8.00 Hz, 2H, Ar-H), 7.57 (t, *J*= 8.00 Hz, 2H, Ar-H), 7.66 (d, *J*=8.00, 2H, Ar-H), 7.72 (d, *J*= 8.00 Hz, 2H, Ar-H), 8.21 (d, *J*= 8.00 Hz, 2H, Ar-H); Elemental analysis calculated for $C_{22}H_{17}ClN_4O$: C 64.41, H 4.73, N 9.39; Found C 64.72, H 4.89, N 9.51.

2-(4-Fluorophenyl)-3-((3,4,5-trimethoxybenzylidene)amino)quinazolin-4(3*H*)-one (15):

White crystals, M.wt. 433.43, Yield: 83.3 %, m.p.: 244-254 °C; FT-IR (KBr) (υ_{max}/ cm^{-1}): 3064 (Ar-H), 2961 (Aliphatic C-H), 1664 (C=O); ^{1}H-NMR ($CDCl_3$): (400 MHz) δ=3.93 (s, 3H, OCH_3), 3.96 (s, 6H, OCH_3), 6.98 (s, 2H, Ar-H), 7.00-8.65 (m, 9H, Ar-H); Elemental analysis calculated for $C_{24}H_{20}FN_3O_4$; C 66.51, H 4.65, N 9.69; Found C 66.72, H 4.69, N 9.84.

2-(4-Fluorophenyl)-3-((2,3,4-trihydroxybenzylidene)amino)quinazolin-4(3*H*)-one (16):

White powder, M.wt. 391.35, Yield: 65.7 %, m.p.: 225-228 °C; FT-IR (KBr) (υ_{max}/ cm^{-1}): 3367 (broad, OH), 3024 (Ar-H), 1687 (C=O); ^{1}H-NMR (DMSO-d_6): (400 MHz) δ= 6.41 (d, *J*=8.00 Hz, 1H, Ar-H), 6.83 (d, *J*=8.00 Hz, 1H, Ar-H), 7.28-7.34 (m, 2H, Ar-H), 7.45 (t, *J*=8.00 Hz, 2H, Ar-H), 7.91-8.18 (m, 2H, Ar-H), 8.53 (d, *J*=8.00 Hz, 2H, Ar-H), 9.58 (s, 1H, N=C*H*), 11.36 (s, 1H, phenolic OH, D_2O exchangeable), 11.94 (s, 1H, phenolic OH, D_2O exchangeable), 12.19 (s, 1H, phenolic OH, D_2O exchangeable); ^{13}C-NMR (DMSO-d_6): (100 MHz) δ= 108.24, 114.73, 116.32, 120.56, 121.67, 123.75, 127.27, 131.43, 131.77, 132.63, 133.10, 139.69, 147.11, 149.49, 151.49, 155.37, 161.71, 164.43,

164.77; Elemental analysis calculated for $C_{21}H_{14}FN_3O_4$: C 64.45, H 3.61, N 10.74; Found C 64.53, H 3.59, N 11.01.

2-(4-Fluorophenyl)-3-((2-hydroxybenzylidene)amino)quinazolin-4(3*H*)-one (17):

White crystals, M.wt. 359.35, Yield: 57 %, m.p.: 193-194 °C; FT-IR (KBr) (υ_{max}/ cm^{-1}): 3385 (broad, OH), 3040 (Ar-H), 1688 (C=O) 1619 (C=C); ^{1}H-NMR ($CDCl_3$): (400 MHz) δ= 7.08-8.41 (m, 12H, Ar-H), 8.70 (s, 1H, N=C*H*), 9.99 (s, 1H, phenolic OH, D_2O exchangeable); Elemental analysis calculated for $C_{21}H_{14}FN_3O_2$: C 70.19, H 3.93, N 11.69; Found C 70.43, H 4.02, N 11.85.

3-((4-Fluorobenzylidene)amino)-2-(4-fluorophenyl)quinazolin-4(3*H*)-one (18):

White powder, M.wt. 361.34, Yield: 82.8 %, m.p.: 174-176 °C; FT-IR (KBr) (υ_{max}/ cm^{-1}): 3071 (Ar-H), 1687 (C=O); ^{1}H-NMR ($CDCl_3$): (400 MHz) δ= 7.18 (t, *J*= 8.00 Hz, 2H, Ar-H), 7.22 (d, *J*= 8.00 Hz, 2H, Ar-H), 7.80-7.90 (m, 4H, Ar-H), 8.12-8.16 (m, 3H, Ar-H), 8.33 (d, *J*= 8.00 Hz, 1H, Ar-H), 8.65 (s, 1H, N=C*H*); Elemental analysis calculated for $C_{21}H_{13}F_2N_3O$: C 69.80, H 3.63, N 11.63; Found C 70.02, H 3.61, N 11.92.

2-(4-Fluorophenyl)-3-((4-hydroxybenzylidene)amino)quinazolin-4(3*H*)-one (19):

Brown powder, M.wt. 359.35, Yield: 63 %, m.p.: 239-242 °C, IR (KBr) (cm^{-1}): 3332 (broad, OH), 3060 (Ar-H), 1692 (C=O); ^{1}H-NMR ($CDCl_3$): (400 MHz) δ= 7.23 (t, *J*= 8.00 Hz, 2H, Ar-H), 7.54-7.64 (m, 3H, Ar-H), 7.83-7.88 (m, 2H, Ar-H), 7.96-8.02 (m, 2H, Ar-H), 8.07 (d, *J*= 8.00 Hz, 2H, Ar-H), 8.34-8.37 (m, 1H, Ar-H), 9.34 (s, 1H, N=C*H*), 10.97 (s, 1H, phenolic OH, D_2O exchangeable); Elemental analysis calculated for $C_{21}H_{14}FN_3O_2$: C 70.19, H 3.93, N 11.69; Found C 70.32, H 3.97, N 11.85.

3-((1-(4-Aminophenyl)ethylidene)amino)-2-(4-fluorophenyl)quinazolin-4(3*H*)-one (20):

Yellow powder, M.wt. 372.39, Yield: 55.5 %, m.p.: 188-190 °C; FT-IR (KBr) (υ_{max}/ cm^{-1}): 3010 (Ar-H), 1689 (C=O); ^{1}H-NMR ($CDCl_3$): (400 MHz) δ= 1.18 (s, 3H, aliphatic CH_3), 5.19 (s, 2H, NH_2, D_2O exchangeable), 7.06 (t, *J*= 8.00 Hz, 2H, Ar-H), 7.48-7.52 (m, 4H, Ar-H), 7.68-7.75 (m, 2H, Ar-H), 7.88-7.92 (m, 2H, Ar-H), 8.00 (d, *J*= 8.00 Hz, 1H, Ar-H), 8.21 (d, *J*= 8.00 Hz, 1H, Ar-H); Elemental analysis calculated for $C_{22}H_{17}FN_4O$: C 70.96, H 4.60, N 15.04; Found C 71.23, H 4.65, N 15.31.

2-(4-Fluorophenyl)-3-((1-(4-(methylsulfonyl)phenyl)ethylidene(amino)quinazolin-4(3*H*)-one (21):

White powder, M.wt. 435.47, Yield: 73.8 %, m.p.: 253-254 °C; FT-IR (KBr) (υ_{max}/ cm^{-1}): 3026 (Ar-H), 2929 (Aliphatic C-H), 1667 (C=O), 1307 (S=O); ^{1}H-NMR (DMSO-d_6): (400 MHz) δ= 1.99 (s, 3H, aliphatic CH_3), 2.48 (s, 3H, -SO_2-C$\underline{H_3}$), 7.44 (d, *J*=8.00, 2H, Ar-H), 7.48 (d, *J*= 8.00 Hz, 2H, Ar-H), 7.57 (t, *J*= 8.00 Hz, 2H, Ar-H), 7.66-7.72 (m, 4H, Ar-H), 8.21 (d, *J*= 8.00 Hz, 2H, Ar-H); Elemental analysis calculated for $C_{22}H_{17}ClN_4O$: C 63.44, H 4.17, N 9.65; Found C 63.25, H 4.12, N 9.88.

2-(4-Chlorophenyl)-3-((3,4,5-trimethoxybenzylidene)amino)quinazolin-4(3*H*)-one (22):

White powder, M.wt. 449.89, Yield: 90.9 %, m.p.: 247-251 °C; FT-IR (KBr) (υ_{max}/ cm^{-1}): 3069 (Ar-H), 2966 (aliphatic C-H), 1650 (C=O), 1603 (C=C); ^{1}H-NMR ($CDCl_3$): (400 MHz) δ=3.93 (s, 3H, OCH_3), 3.96 (s, 6H, OCH_3), 7.00 (t, *J*= 8.00 Hz, 2H, Ar-H), 7.07 (s, 2H, Ar-H), 7.51-8.00 (m, 6H, Ar-H), 8.57 (ds, 1H, N=C*H*); Elemental analysis calculated for $C_{24}H_{20}ClN_3O_4$: C 64.07, H 4.48, N 9.34; Found C 64.24, H 4.56, N 9.57.

2-(4-Chlorophenyl)-3-((2,3,4-trihydroxybenzylidene)amino)quinazolin-4(3*H*)-one (23):

White powder, M.wt. 407.81, Yield: 52.5 %, m.p.: 230-234 °C; FT-IR (KBr) (υ_{max}/ cm^{-1}): 3323 (broad, OH), 3080 (Ar-H), 2989 (Aliphatic C-H), 1684 (C=O); ^{1}H-NMR (DMSO-d_6): (400 MHz) δ= 6.44-6.51 (m, 2H, Ar-H), 6.93 (d, *J*=8.00 Hz, 2H, Ar-H), 7.52-7.81 (m, 3H, Ar-H), 8.19 (d, *J*=8.00 Hz, 2H, Ar-H), 8.53 (d, *J*=8.00 Hz, 1H, Ar-H), 8.93 (s, 1H, N=C*H*), 11.30 (s, 1H, phenolic OH, D_2O exchangeable), 11.95 (s, 1H, phenolic OH, D_2O exchangeable), 12.20 (s, 1H, phenolic OH, D_2O exchangeable); ^{13}C-NMR (DMSO-d_6): (100 MHz) δ=108.86, 111.29, 115.95, 120.97, 121.68, 122.40, 126.52, 127.93, 127.92, 127.96, 129.44, 133.15, 133.72, 134.151, 148.10, 151.73, 155.33, 158.45, 161.67; Elemental analysis calculated for $C_{21}H_{14}ClN_3O_4$: C 61.85, H 3.46, N 10.30; Found C 62.01, H 3.49, N 10.47.

2-(4-Chlorophenyl)-3-((2-hydroxybenzylidene)amino)quinazolin-4(3*H*)-one (24):

White powder, M.wt. 375.81, Yield: 56.7 %, m.p.: 248-250 °C; FT-IR (KBr) (υ_{max}/ cm^{-1}): 3309 (broad, OH), 3060 (Ar-H), 1682 (C=O); ^{1}H-NMR ($CDCl_3$): (400 MHz) δ= 6.92-7.50 (m, 6H, Ar-H), 7.90 (d, *J*= 8.00 Hz, 2H, Ar-H), 7.9-8.51 (m, 4H, Ar-H), 9.83 (ds, 1H, N=C*H*), 10.95 (s, 1H, phenolic OH, D_2O exchangeable); Elemental analysis calculated for $C_{21}H_{14}ClN_3O_2$: C 67.12, H 3.75, N 11.18; Found C 67.28, H 3.74, N 11.37.

2-(4-Chlorophenyl)-3-((4-fluorobenzylidene)amino)quinazolin-4(3*H*)-one (25):

Yellowish white powder, M.wt. 377.80, Yield: 83.7 %, m.p.: 252-254 °C; FT-IR (KBr) (υ_{max}/ cm^{-1}): 3054 (Ar-H), 1684 (C=O); ^{1}H-NMR ($CDCl_3$): (400 MHz) δ= 7.15-7.21 (m, 2H, Ar-H), 7.24 (t, *J*= 8.00 Hz, 2H, Ar-H), 7.49-7.53 (m, 3H, Ar-H), 7.92-9.96 (m, 2H, Ar-H), 8.03 (d, *J*= 8.00 Hz, 1H, Ar-H), 8.29 (d, *J*= 8.00 Hz, 2H, Ar-H) 8.9 (ds, 1H, N=C*H*); Elemental analysis calculated for $C_{21}H_{13}ClFN_3O$: C 66.76, H 3.47, N 11.12; Found C 66.89, H 3.49, N 11.34.

2-(4-Chlorophenyl)-3-((4-hydroxybenzylidene)amino)quinazolin-4(3*H*)-one (26):

Brownish white powder, M.wt. 375.81, Yield: 67.6 %, m.p.: 250-252 °C; FT-IR (KBr) (υ_{max}/ cm^{-1}): 3325 (broad, OH), 3078 (Ar-H), 1684 (C=O); ^{1}H-NMR ($CDCl_3$): (400 MHz) δ= 6.97 (d, *J*= 8.00 Hz, 3H, Ar-H), 7.51-7.54 (m, 2H, Ar-H), 7.62 (t, *J*= 8.00 Hz, 1H, Ar-H), 7.83 (d, *J*= 8.00 Hz, 3H, Ar-H), 7.90-7.94 (m, 2H, Ar-H), 8.11 (t, *J*= 8.00 Hz, 1H, Ar-H), 8.35 (ds, 1H, N=C*H*), 10.54 (s, 1H, phenolic OH, D_2O exchangeable); Elemental analysis calculated for $C_{21}H_{14}ClN_3O_2$: C 67.12, H 3.75, N 11.18; Found C 67.30, H 3.72, N 11.32.

3-((1-(4-Aminophenyl)ethylidene)amino)-2-(4-chlorophenyl)quinazolin-4(3*H*)-one (27):

White powder, M.wt. 388.85, Yield: 55.2 %, m.p.: 193-195 °C; FT-IR (KBr) (υ_{max}/ cm^{-1}): 3010 (Ar-H), 1689 (C=O); ^{1}H-NMR ($CDCl_3$): (400 MHz) δ= 1.27 (s, 3H, aliphatic CH_3), 5.16 (s, 2H, NH_2, D_2O exchangeable), 7.47 (d, *J*= 8.00 Hz, 2H, Ar-H), 7.58 (t, *J*= 8.00 Hz, 1H, Ar-H), 7.79-7.81 (m, 1H, Ar-H), 7.87 (d, *J*= 8.00 Hz, 4H, Ar-H), 7.97 (d, *J*= 8.00 Hz, 2H, Ar-H), 8.32 (d, *J*= 8.00 Hz, 2H, Ar-H); Elemental analysis calculated for $C_{22}H_{17}ClN_4O$: C 67.95, H 4.41, N 14.41; Found C 68.13, H 4.48, N 14.63.

2-(4-Chlorophenyl)-3-((1-(4-(methylsulfonyl)phenyl)ethylidene(amino)quinazolin-4(3*H*)-one (28):

White powder, M.wt. 451.93, Yield: 66.6 %, m.p.: 241-243 °C; FT-IR (KBr) (υ_{max}/ cm^{-1}): 3007 (Ar-H), 2925 (Aliphatic C-H), 1672 (C=O); ^{1}H-NMR (DMSO-d_6): (400 MHz) δ= 1.99 (s, 3H, aliphatic CH_3), 2.48 (s, 3H, -SO_2-C<u>H</u>$_3$), 7.44 (d, *J*=8.00, 2H, Ar-H), 7.48 (d, *J*= 8.00 Hz, 2H, Ar-H), 7.57 (t, *J*= 8.00 Hz, 2H, Ar-H), 7.66 (d, *J*=8.00, 2H, Ar-H), 7.72 (d, *J*= 8.00 Hz, 2H, Ar-H), 8.21 (d, *J*= 8.00 Hz, 2H, Ar-H); Elemental analysis calculated for $C_{22}H_{17}ClN_4O$: C 61.13, H 4.01, N 9.30; Found C 61.50, H 4.18, N 9.16.

7-Chloro-2-(4-methoxyphenyl)-3-((2,3,4-trihydroxybenzylidene)amino)quinazolin-4(3*H*)-one (29):

Yellowish white powder, M.wt. 437.83, Yield: 74 %, m.p.: 225-227 °C; FT-IR (KBr) (υ_{max}/ cm^{-1}): 3445 (broad, OH), 3055 (Ar-H), 2975 (Aliphatic C-H), 1638 (C=O); ^{1}H-NMR (DMSO-d_6): (400 MHz) δ= 3.85 (s, 3H, OCH_3), 6.46 (d, *J*=8.00 Hz, 2H, Ar-H), 6.93-7.03 (m, 2H, Ar-H), 7.53 (d, *J*=8.00 Hz, 2H, Ar-H), 7.73 (s,1H, Ar-H), 7.85 (d, *J*=8.00 Hz, 1H, Ar-H), 7.98 (d, *J*=8.00 Hz, 1H, Ar-H), 8.76 (s, 1H, N=C*H*), 11.37 (s, 1H, phenolic OH, D_2O exchangeable), 11.89 (s, 1H, phenolic OH, D_2O exchangeable), 12.29 (s, 1H, phenolic OH, D_2O exchangeable); ^{13}C-NMR (DMSO-d_6): (100 MHz) δ=55.96, 108.60, 111.17, 113.25, 118.98, 120.28, 121.69, 122.91, 123.46, 126.49, 126.77, 128.58, 129.50, 131.99, 132.22, 133.22, 150.62, 151.83, 157.07, 161.29; Elemental analysis calculated for $C_{22}H_{16}ClN_3O_5$: C 60.35, H 3.68, N 9.60; Found C 60.48, H 3.52, N 9.78.

4-(4-Oxo-3-((2,3,4-trihydroxybenzylidene)amino)-3,4-dihydroquinazolin-2-yl)benzonitrile (30):

Yellowish white powder, M.wt. 398.37, Yield: 43.6 %, m.p.: 145-147 °C; FT-IR (KBr) (υ_{max}/ cm^{-1}): 3320 (broad, OH), 3113 (Ar-H), 2231 (C≡N), 1648 (C=O); ^{1}H-NMR (DMSO-d_6): (400 MHz) δ= 6.90 (d, *J*=8.00 Hz, 2H, Ar-H), 7.10 (d, *J*=8.00 Hz, 2H, Ar-H), 7.45-7.85 (m,4H, Ar-H), 8.22 (d, *J*=8.00 Hz, 1H, Ar-H), 8.24 (d, *J*=8.00 Hz, 1H, Ar-H), 8.91 (s, 1H, N=C*H*), 10.22 (s, 1H, phenolic OH, D_2O exchangeable), 10.56 (s, 1H, phenolic OH, D_2O exchangeable), 10.87 (s, 1H, phenolic OH, D_2O exchangeable); ^{13}C-NMR (DMSO-d_6): (100 MHz) δ=115.85, 120.44, 121.49, 122.99, 124.60, 126.49, 127.16, 127.32, 127.63, 127.82, 127.94, 128.37, 129.74, 129.97,

130.02, 130.09, 135.22, 149.37, 158.54, 161.74; Elemental analysis calculated for $C_{22}H_{14}N_4O_4$: C 66.33, H 3.54, N 14.06; Found C 66.45, H 3.40, N 14.34.

3-((2,3,4-Trihydroxybenzylidene)amino)-2-(3,4,5-trimethoxyphenyl)quinazolin-4(3*H*)-one (31):

Yellowish white powder, M.wt. 463.44, yield: 70 %, m.p.: 265-267 °C; FT-IR (KBr) (υ_{max}/ cm^{-1}):3340 (broad, OH), 3063 (Ar-H), 2955 (Aliphatic C-H), 1661 (C=O); ^{1}H-NMR (DMSO-d_6): (400 MHz) δ= 3.54 (s, 3H, OCH_3), 3.82 (s, 6H, OCH_3), 6.94 (d, *J*= 8.00 Hz, 1H, Ar-H), *7*.11 (s, 2H, Ar-H), 7.58 (t, *J*= 8.00 Hz, 1H, Ar-H), 7.72 (d, *J*= 8.00 Hz, 1H, Ar-H), 7.85 (t, *J*= 8.00 Hz, 1H, Ar-H), 8.20 (d, *J*= 8.00 Hz, 2H, Ar-H), 8.75 (s, 1H, N=C*H*), 10.20 (s, 1H, phenolic OH, D_2O exchangeable), 11.24 (s, 1H, phenolic OH, D_2O exchangeable), 11.52 (s, 1H, phenolic OH, D_2O exchangeable); ^{13}C-NMR (DMSO-d_6): (100 MHz) δ=56.61, 60.59, 107.82, 111.19, 112.56, 119.46 120.43, 123.40, 126.50, 127.21, 127.87, 130.64, 132.88, 139.10, 144.78, 146.89, 149.74, 150.68, 152.54, 155.97, 161.57 ; Elemental analysis calculated for $C_{24}H_{21}N_3O_7$: C 62.20, H 4.57, N 9.07; Found C 62.49, H 4.68, N 8.79.

2-(4-Nitrophenyl)-3-((2,3,4-trihydroxybenzylidene)amino)quinazolin-4(3*H*)-one (32):

Yellowish white powder, M.wt. 418.36, yield: 56.5 %, m.p.: 191-194 °C; FT-IR (KBr) (υ_{max}/ cm^{-1}): 3446 (broad, OH), 3037 (Ar-H), 2928 (Aliphatic C-H), 1647 (C=O); ^{1}H-NMR (DMSO-d_6): (400 MHz) δ= 6.83 (d, *J*= 8.00 Hz, 2H, Ar-H), 6.93 (d, *J*= 8.00 Hz, 2H, Ar-H), 7.10 (d, *J*= 8.00 Hz, 1H, Ar-H), 7.27-8.02 (m, 5H, Ar-H), 8.93 (s, 1H, N=C*H*), 11.35 (s, 1H, phenolic OH, D_2O exchangeable), 11.91 (s, 1H, phenolic OH, D_2O exchangeable), 12.24 (s, 1H, phenolic OH, D_2O exchangeable); ^{13}C-NMR (DMSO-d_6): (100 MHz) δ=108.82, 111.27, 114.96, 116.54, 120.84, 121.63, 122.54, 127.29, 130.30, 132.62, 139.63, 147.09, 149.47, 151.52, 152.77, 153.76, 155.38, 158.49, 161.73; Elemental analysis calculated for $C_{21}H_{14}N_4O_6$: C 60.29, H 3.37, N 13.39; Found C 60.43, H 3.26, N 12.94.

7-Chloro-2-(4-fluorophenyl)-3-((2,3,4-trihydroxybenzylidene)amino)quinazolin-4(3*H*)-one (33):

Yellowish white powder, M.wt. 425.80, yield: 61 %, m.p.: 248-250 °C; FT-IR (KBr) (υ_{max}/ cm^{-1}): 3335 (broad, OH), 2919 (Aliphatic C-H), 1648 (C=O); ^{1}H-NMR (DMSO-d_6): (400 MHz) δ= 6.28 (d, *J*= 8.00 Hz, 2H, Ar-H), 6.43-6.51 (m, 4H, Ar-H), 7.10 (d, *J*= 8.00 Hz, 1H, Ar-H), 7.81 (s, 1H, Ar-H), 8.19 (d, *J*= 8.00 Hz, 2H, Ar-H), 8.75 (s, 1H, N=C*H*), 10.23 (s, 1H, phenolic OH, D_2O exchangeable), 11.53 (s, 1H, phenolic OH, D_2O exchangeable), 11.55 (s, 1H, phenolic OH, D_2O exchangeable); ^{13}C-NMR (DMSO-d_6): (100 MHz) δ=107.30, 108.57, 111.18, 112.56, 114.79, 119.47, 123.41, 127.58, 128,66, 132.71, 132.87, 133.04, 144.79, 146.89, 147.02, 149.08, 150.63, 161.25, 163.28; Elemental analysis calculated for $C_{21}H_{13}ClFN_3O_4$: C 59.24, H 3.08, N 9.87; Found C 59.66, H 3.16, N 10.35.

2.2 *Biological Evaluation*

2.2.1 *PDE 4 inhibition Assay*

PDE assays were performed using commercially available purified or recombinant enzyme. Enzyme activity was determined through titration in order to determine the concentration of enzyme required to produce 80% activity (EC_{80}). Compounds of interest were pre-incubated with appropriate concentrations of enzymes to allow compound to enzyme binding for 30 minutes. Fluorescently labeled cGMP or cAMP were then added and allowed to incubate for 1.5 hours. The experiments were terminated through the addition of binding buffer containing beads that bind to the linearized 5'GMP or 5'AMP and fluorescence polarization is measured through polarized excitation at 485 nM and emission was measured at 528 nM in parallel and perpendicular orientations. Unbound and unhydrolyzed substrate has a higher rotation in solution which corresponds to a lower polarization than bound product. These values are then normalized to vehicle control wells before being analyzed by nonlinear regression [14].

2.2.2 *In Vitro Anti-Lung Cancer and Anti Colon Cancer Assays:*

Compounds were analyzed for cancer cell growth inhibitory activity. These studies were carried out using cells derived from human lung tumors (A549-cells) and colon tumors (HT-29 cells) at USA Mitchell Cancer Institute Drug Discovery Laboratory, University of South Alabama. This assessment of activity tested each compound in quadruplicate at a

maximum concentration of 50 µM, followed by 6 serially diluted concentrations [15].

A549-cells were obtained from 90-95% joining 10 cm dishes, and diluted in growth medium. Then, appropriate concentration of cells to were prepared to add cells in a volume of 25 µL per well in tissue culture treated Griener 384-well microplates, then incubated overnight at 37°C.

Compounds were diluted to a concentration of 50 mM in DMSO. Concentrated dosing solutions of twice the final concentration were prepared by dilution of the DMSO stocks 1:500 in growth media. Serial dilutions twice were then prepared in medium containing 0.2 % DMSO to maintain a suitable concentration of vehicle into the concentration range of the compound. Each of these was added in equal volume (25 µL), to four wells on the cell assay plate, along with vehicle control. Cells were incubated with the compounds for a further 3 days.

At the end of this period, assay plates were allowed to cool to room temperature for 10 min prior to addition of 25 µL per well Promega CellTiter Glo reagent, followed by an additional 10 min incubation. The resulting luminescence was quantitated using a Molecular Devices Spectramax Paradigm.

% growth inhibition was calculated as, where 100% represents the viability of vehicle treated control samples:

$$100 - \left(100 \times \frac{\text{(sample)}}{\text{(Vehicle control)}}\right)$$

Thus, on average, growth inhibition of vehicle control samples equals zero.

Potency of compounds was determined using the Non Linear Dose Response algorithm (4-parameter logistic fit) with GraphPad Prism 5 software.

2.2.3 ***Molecular Modeling Study***

The 3D structures of the compounds were built by using the MOE 2018.0101 of (Chemical Computing Group Inc software, Canada) drawing tool bar. The Lowest energy conformer of the compounds (global-minima) was docked into the active site of PDE 4B, which is in a complex with pyrano[3,2-*d*]pyrimidine derivative (**PDB ID: 3W5E**). The LigX option was used to structure preparation, correction, and 3D protonation with refinement RMSD gradient to 0.1 kcal/mol/Å. The molecular mechanics force field 'MMFF94x' was used to energy minimization for each compound. The compounds were docked in the same pocket of the pyrano[3,2-*d*]pyrimidine derivative. Energy of binding was calculated as the difference between the energy of the complex and individual energies of the enzyme and ligand. The compounds under study were subjected to flexible alignment experiment using 'Molecular Operating Environment' software (MOE of Chemical Computing Group Inc., on a Core i5 2.2 GHz workstation). The molecules were constructed using the Builder module of MOE. Their geometry was optimized by using the MMFF94 forcefield followed by a flexible alignment using systematic conformational search. . The Lowest energy aligned conformers were identified [16].

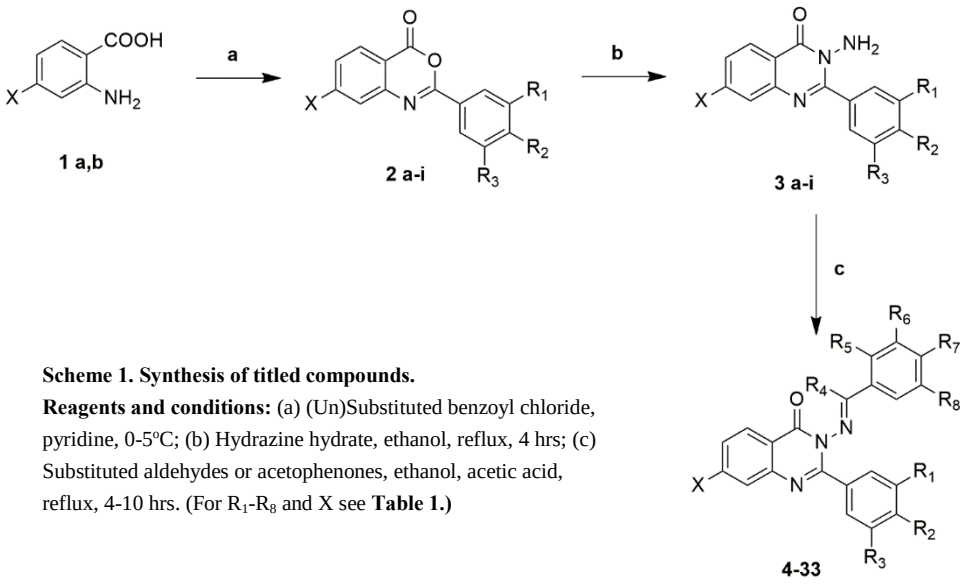

Scheme 1. Synthesis of titled compounds.
Reagents and conditions: (a) (Un)Substituted benzoyl chloride, pyridine, 0-5°C; (b) Hydrazine hydrate, ethanol, reflux, 4 hrs; (c) Substituted aldehydes or acetophenones, ethanol, acetic acid, reflux, 4-10 hrs. (For R_1-R_8 and X see **Table 1.)**

3. **Results and Discussion**

3.1 *Chemistry*

The title compounds **4-33** were synthesized and outlined in **Scheme 1**. Reaction of anthranilic acid **1a** or 5-chloro anthranilic acid **1b** with (un)substituted benzoyl chlorides yielded compounds **2a-i** by *N*-acylation via a dehydrative cyclization mechanism [13,17]. Subsequently, heating compounds **2a-i** with hydrazine monohydrate in ethanol under reflux afforded the corresponding amino derivatives **3a-i**, in good yields. Finally, condensation of compounds **3a-i** with different substituted aromatic aldehydes or acetophenones afforded the corresponding titled final compounds **4-33**. Structural elucidation of the synthesized products was confirmed by the aid of elementary analyses, IR spectroscopy, ^{1}H-NMR and ^{13}C-NMR spectroscopy. The obtained data agreed with the proposed structures. Moreover, molecular docking studies for some selected representative compounds were performed to investigate their binding modes with the active site.

3.2 *Biological Evaluation*

3.2.1 *PDE 4B inhibitory activity*

Compounds **4-33** were assayed for their *in vitro* inhibition of recombinant PDE 4B. Rolipram was used as a positive reference for PDE4 inhibition. Initial screening of the compounds was done at 10 µM in triplicate [14]. Compounds **9, 16, 23, 29, 30, 31, 32 and 33** showed the highest inhibitory activity (% inhibition= 56.05, 85.07, 79.20, 85.36, 62.06, 61.75, 74.64 and 89.07, respectively)**, Table 1.**

Structure activity correlation revealed that PDE 4B inhibitory activity is embedded in the structure core of the most active compounds. Their common structure feature was the 2,3,4-trihydroxy moiety that served as a hydrogen bond donor. The absence of this moiety in the other tested compounds showed a dramatic drop in the inhibitory activity especially in compounds **4, 8, 15** and **22,** which possessed a 3,4,5-trimethoxy moiety (% inhibition= 13.43, 9.38, 3.41 and 2.61, respectively). 2,3,4-trihydroxy moiety as hydrophilic groups on phenyl ring may orient the rest of the ligand towards the polar binding site contain Gln 443 key amino acid. Also, the presence of a chloro group at the benzo moiety of quinazolinone scaffold in compounds **29** and **33** (% inhibition= 85.36 and 89.07, respectively) showed excellent potency, if compared to other active compounds.

3.2.2 *Anti-lung cancer activity*

The most active PDE 4B inhibitors **9, 16, 23, 29, 30, 31, 32 and 33** underwent further antitumor screening assay utilizing human tumor cell lines A549 non-small cell lung cancer (NSCLC) with Doxorubicin as the positive control [15]. **Table 2.** Compounds **16** and **23** showed the highest potency (IC_{50} = 1.55 and 1.30 µM**,** respectively). The results may be due to substitution by small lipophilic group such as F and Cl as well as un-substituted benzo moiety of quinazolinone scaffold. These two factors may affect the uptake of the molecules by cancer cells.

Table 1. In vitro PDE 4B inhibition activity (% inhibition) at 10 µM concentration of the synthesized compounds (4-33).

Compound Number	X	R_1 & R_3	R_2	R_4	R_5	R_6	R_7	R_8	% inhibition [a]
4	H	H	H	H	H	OCH_3	OCH_3	OCH_3	13.43 ± 0.03
5	H	H	H	H	H	H	F	H	16.30 ± 0.02
6	H	H	H	CH_3	H	H	NH_2	H	11.83 ± 0.01
7	H	H	H	CH_3	H	H	SO_2CH_3	H	18.43 ± 0.02
8	H	H	OCH_3	H	H	OCH_3	OCH_3	OCH_3	9.38 ± 0.002
9	H	H	OCH_3	H	OH	OH	OH	H	56.05 ± 0.5
10	H	H	OCH_3	H	OH	H	H	H	16.73 ± 0.03
11	H	H	OCH_3	H	H	H	F	H	4.90 ± 0.01
12	H	H	OCH_3	H	H	H	OH	H	10.87 ± 0.02
13	H	H	OCH_3	CH_3	H	H	NH_2	H	8.20 ± 0.04
14	H	H	OCH_3	CH_3	H	H	SO_2CH_3	H	15.66 ± 0.02
15	H	H	F	H	H	OCH_3	OCH_3	OCH_3	3.41 ± 0.03
16	H	H	F	H	OH	OH	OH	H	85.07 ± 0.55
17	H	H	F	H	OH	H	H	H	9.59 ± 0.01
18	H	H	F	H	H	H	F	H	14.70 ± 0.03
19	H	H	F	H	H	H	OH	H	17.90 ± 0.02
20	H	H	F	CH_3	H	H	NH_2	H	20.25 ± 0.04
21	H	H	F	CH_3	H	H	SO_2CH_3	H	16.58 ± 0.02
22	H	H	Cl	H	H	OCH_3	OCH_3	OCH_3	2.61 ± 0.01
23	H	H	Cl	H	OH	OH	OH	H	79.20 ± 0.42
24	H	H	Cl	H	OH	H	H	H	4.77 ± 0.02
25	H	H	Cl	H	H	H	F	H	2.50 ± 0.01
26	H	H	Cl	H	H	H	OH	H	10.68 ± 0.02
27	H	H	Cl	CH_3	H	H	NH_2	H	7.95 ± 0.01
28	H	H	Cl	CH_3	H	H	SO_2CH_3	H	12.83 ± 0.01
29	Cl	H	OCH_3	H	OH	OH	OH	H	85.36 ± 0.6
30	H	H	CN	H	OH	OH	OH	H	62.06 ± 0.15
31	H	OCH_3	OCH_3	H	OH	OH	OH	H	61.75 ± 0.2
32	H	H	NO_2	H	OH	OH	OH	H	74.64 ± 0.23
33	Cl	H	F	H	OH	OH	OH	H	89.07 ± 0.5
Rolipram (150 nM)									50.00 ± 0.1

[a] Data are presented as the means ± SDs of three independent experiment

3.2.3 *Anti-colon cancer activity*

Also, the same compounds were subjected to antitumor screening assay using human colon tumor cell line HT-29 cells including Doxorubicin as the positive control, where compound **16** showed the highest potency (IC_{50}= 0.6 µM) [18]. **Table 2.**

3.3 *Molecular Modeling Study and Computational Analysis*

3.3.1 *Molecular Modeling Study*

Table 2. Growth inhibition of cancer cell lines (IC_{50}, µM) of compounds with the highest PDE 4B % inhibition.

Compounds	A549 Lung Cancer cell lines [IC_{50} (µM)][a]	HT-29 Colon Cancer cell lines [IC_{50} (µM)]
9	2.2 ± 0.2	1.1 ±0.1
16	1.6 ± 0.1	0.6 ±0.2
23	1.3 ±0.1	1.1 ±0.1
29	4.3 ±0.2	9.9 ±0.2
30	3.2 ±0.4	5.5 ±0.3
31	5.4 ±0.02	8.7 ±0.6
32	2.2 ±0.2	6.0 ±0.5
33	5.9 ±0.1	8.6 ±0.7
Doxorubicin	0.11 ±0.01	0.3 ±0.02

[a] Data are presented as the means ± SDs of three independent experiments.

Docking studies for the most active compound **33** have been performed using the MMFF94 force-field implemented in Molecular Operating Environment (MOE 2018.0101) developed by Chemical Computing Group. Docking studies were made using PDE4B co-crystallized with a thiopyrano[3,2-*d*]pyrimidine ligand (PDB ID: **3W5E**). Docking validation was performed by docking the co-crystallized ligand showed root mean square deviation (rmsd) of 0.875 between the docked pose and the co-crystallized ligand. Fifty poses of compound **33** were scored by initial rescoring methodology (London dG) and the final re-scoring methodology (GVBI/WSA dG) after placement using Triangle Matcher and post-placement refinement was Force Field.

Compound **33** has shown significant good affinity and binding interactions to the essential amino acid residues needed for PDE 4B inhibition. It underwent a hydrogen bond between Gln 443 and the quinazoline nitrogen moiety that acted as a hydrogen bond acceptor (bond length 3.66 Å), a hydrophobic interaction with Phe 446 and a third bond between Tyr 403 and the chloro moiety (halogen bond length 4.01 Å)**, (Fig. 4).** On the other hand, the least active compounds did not show any interaction with the previously mentioned residues in the active site of the target enzyme. It could be noticed that the common feature of these compounds is absence of tri-hydroxy moiety and chloro moiety at benzo ring of the quinazoline scaffold, the fact that may lead to a different orientation, far from the key amino acids.

3.3.2 *Computational Analysis*

3.3.2.1 *Physicochemical Parameters*

Computational study for the prediction of

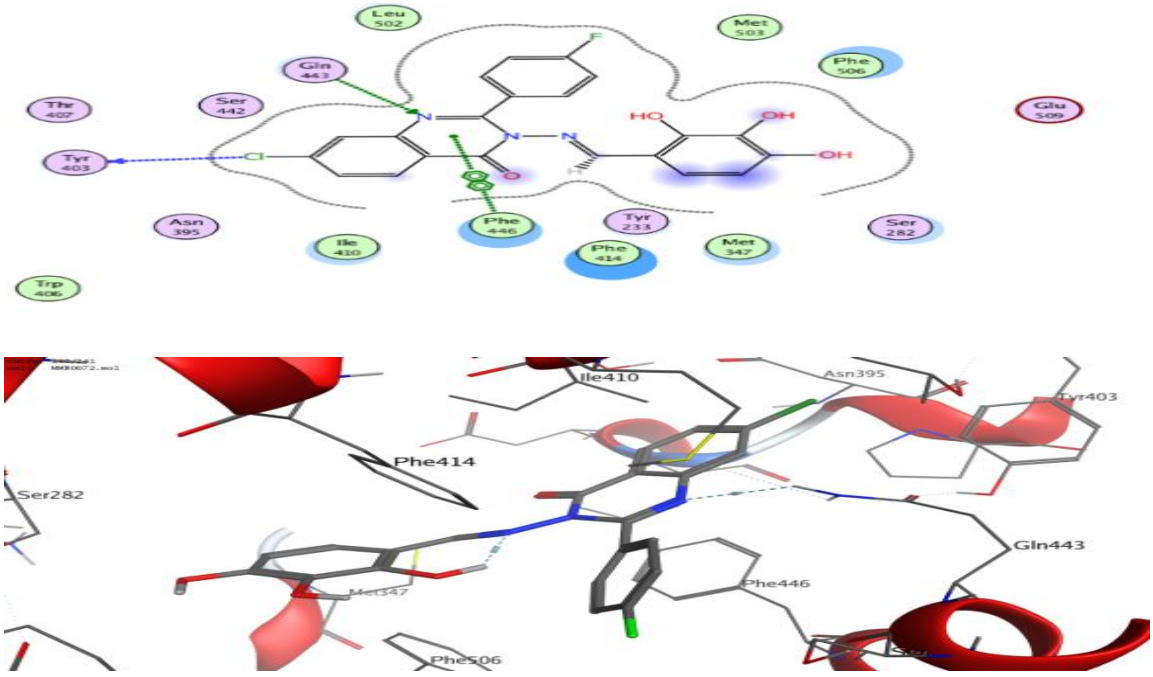

Figure 4: Docking pose of compound 33 in PDE4B active site.

physicochemical parameters of the most active compounds **9, 16, 23, 29, 30, 31, 32 and 33** were hydrogen bond acceptors and donor atoms of 'Lipinski's rule of five' [19], number of rotatable bonds and molecular polar surface area were calculated using the Molinspiration online property calculation [20].

The computed molecular properties were recorded in **Table 3**. Lipinski's rule, topological polar surface area (TPSA) and number of rotatable bonds (Nrotb) are the most important characteristics for prediction of the oral bioavailability of the compounds in humans. Compounds **9, 16, 23, 29, 30, 31, 32 and 33** are compatible with parameters of these rules. Accordingly, such compounds may have good bioavailability parameters.

Table 3. Calculated Lipinski's rule, TPSA and Nrotb for the most active compounds. Calculated using Molinspiration online property calculation**.**

Compound Number	miLogP	M. wt.	nOH-NH	nO-N	TPSA	Nrotb	No. of violations
9	3.63	403.39	3	8	117.18	4	0
16	3.74	391.36	3	7	107.94	3	0
23	4.25	407.81	3	7	107.94	3	0
29	4.28	437.84	3	8	117.18	4	0
30	3.33	398.38	3	8	131.74	3	0
31	3.20	463.45	3	10	135.65	6	0
32	3.53	418.37	3	10	153.77	4	0
33	4.39	425.80	3	7	107.94	3	0

**miLogP: Partition co-efficient, M.wt.: Molecular weight, nOH-NH: Number of hydrogen bond donors, nO-N: Number of hydrogen bond acceptors, TPSA: Total polar surface area and Nrotb: Number of rotatable bonds.

3.3.2.2 *Drug-likeness and toxicity tendencies*

Calculation of drug-likeness properties and toxicity hazards of the most active compounds **9, 16, 23, 29, 30, 31, 32 and 33** were made by Data Warrior software developed by Osiris [21]. **Table 4**. The compounds demonstrated positive values to be Drug-like agents, except for compound **30** that scored -0.44169 and compound **32** that scored -1.3374. This may be attributed to -C≡N and $–NO_2$ moieties, respectively.

Fortunately, the most active compounds have passed the test for mutagenicity, tumorigenicity or irritation tendencies with the software with negative results and thus may be safe for human administration following preclinical testing.

4. Conclusion

Together, the docking simulation study, along with the *in vitro* assay results, demonstrated that the newly synthesized compounds **9, 16, 23, 29, 30, 31, 32 and 33** may serve as good PDE 4B inhibitors, notably compounds **29** and **33** (% inhibition= 85.36 and 89.07 at 10 µM**,** respectively) if compared to rolipram. These findings support such compounds to act as promising drug candidates for the treatment of COPD and lung cancer. Also, compounds **16** and **23** showed the highest anti- lung cancer potency (IC_{50} = 1.55 and 1.30 µM**,** respectively), if compared to doxorubicin (IC_{50} = 0.11 µM). The selected

Table 4. Calculated values of Drug-likeness values and expected Toxicity tendencies, all calculated by Data Warrior software developed by Osiris Software.

Compound Number	Drug-likeness	Toxicity Tendencies		
		Mutagenicity	Tumorigenicity	Irritation
9	3.7685	None	None	None
16	2.4983	None	None	None
23	3.8605	None	None	None
29	3.8043	None	None	None
30	-0.44169	None	None	None
31	3.7685	None	None	None
32	-1.3374	None	None	None
33	2.5205	None	None	None

compounds showed good to moderate activities against colon cancer, especially compound **16**, which was the most potent (IC_{50}= 0.6 µM). Moreover, those compounds obeyed Lipinski's rule of five, so they are expected to demonstrate good oral absorption. Additionally, the same tested compounds have passed the tests of drug-likeness properties and toxicity hazards with no mutagenicity, tumorigenicity or irritation tendencies, expect for compound **30** that scored -0.44169 and compound **32** that scored -1.3374 in drug-likeness test. Compounds **9, 16, 23, 29, 30, 31, 32 and 33** may serve as safe therapeutic candidates for preclinical evaluation.

5. Conflicts of interest

No potential conflicts of interest are reported by the authors.

6. References

1. Copur, M. S. (2019). State of cancer research around the globe. *Oncology*, *33*(5).

2. Koulenti, D., Parisella, F. R., Xu, E., Lipman, J., & Rello, J. (2019). The relationship between ventilator-associated pneumonia and chronic obstructive pulmonary disease: what is the current evidence?. *European Journal of Clinical Microbiology & Infectious Diseases*, *38*(4), 637-647.

3. Durham, A. L., & Adcock, I. M. (2015). The relationship between COPD and lung cancer. *Lung Cancer*, *90*(2), 121-127.

4. Kümmerle, A. E., Schmitt, M., Cardozo, S. V., Lugnier, C., Villa, P., Lopes, A. B., ... & Bourguignon, J. J. (2012). Design, synthesis, and pharmacological evaluation of N-acylhydrazones and novel conformationally constrained compounds as selective and potent orally active phosphodiesterase-4 inhibitors. *Journal of medicinal chemistry*, *55*(17), 7525-7545.

5. Abdel-Rahman, H. M., Abdel-Aziz, M., Canzoneri, J. C., Gary, B. D., & Piazza, G. A. (2014). Novel Quinazolin-4 (3H)-one/Schiff Base Hybrids as Antiproliferative and Phosphodiesterase 4 Inhibitors: Design, Synthesis, and Docking Studies. *Archiv der Pharmazie*, *347*(9), 650-657.

6. AZAM, M., & TRIPURANENI, N. (2014). Selective phosphodiesterase 4B inhibitors: a review. *Scientia pharmaceutica*, *82*(3), 453-482.

7. Savai, R., Pullamsetti, S. S., Banat, G. A., Weissmann, N., Ghofrani, H. A., Grimminger, F., & Schermuly, R. T. (2010). Targeting cancer with phosphodiesterase inhibitors. *Expert opinion on investigational drugs*, *19*(1), 117-131.

8. Maurice, D. H., Ke, H., Ahmad, F., Wang, Y., Chung, J., & Manganiello, V. C. (2014). Advances in targeting cyclic nucleotide phosphodiesterases. *Nature reviews Drug discovery*, *13*(4), 290.

9. Barnes, P. J. (2013). Theophylline. *American journal of respiratory and critical care medicine*, *188*(8), 901-906.

10. da Costa Nunes, I. K., de Souza, E. T., Cardozo, S. V. S., de Frias Carvalho, V., Romeiro, N. C., e Silva, P. M. R., ... & Lima, L. M. (2016). Synthesis, pharmacological profile and docking studies of new sulfonamides designed as phosphodiesterase-4 inhibitors. *PloS one*, *11*(10).

11. Dal Piaz, V., & Giovannoni, M. P. (2000). Phosphodiesterase 4 inhibitors, structurally unrelated to rolipram, as promising agents for the treatment of asthma and other pathologies. *European journal of medicinal chemistry*, *35*(5), 463-480.

12. Abdel-Rahman, H. M., Abdel-Aziz, M., Tinsley, H. N., Gary, B. D., Canzoneri, J. C., & Piazza, G. A. (2016). Design and Synthesis of Substituted Pyridazinone-1-Acetylhydrazones as Novel Phosphodiesterase 4 Inhibitors. *Archiv der Pharmazie*, *349*(2), 104-111.

13. Kumar, K. S., Ganguly, S., Veerasamy, R., & De Clercq, E. (2010). Synthesis, antiviral activity and cytotoxicity evaluation of Schiff bases of some 2-phenyl quinazoline-4 (3) H-ones. *European journal of medicinal chemistry*, *45*(11), 5474-5479.

14. Rybalkin, S. D., Hinds, T. R., & Beavo, J. A. (2013). Enzyme assays for cGMP hydrolyzing phosphodiesterases. In *Guanylate Cyclase and Cyclic GMP* (pp. 51-62). Humana Press, Totowa, NJ.

15. Xie, J., Liu, J., Liu, H., Liang, S., Lin, M., Gu, Y., ... & Mo, S. L. (2015). The antitumor effect of tanshinone IIA on anti-proliferation and decreasing VEGF/VEGFR2 expression on the human non-small cell lung cancer A549 cell line. *Acta pharmaceutica Sinica B*, *5*(6), 554-563.

16. Goto, T., Shiina, A., Yoshino, T., Mizukami, K., Hirahara, K., Suzuki, O., ... & Takahashi, M. (2013). Identification of the fused bicyclic 4-amino-2-phenylpyrimidine derivatives as novel and potent PDE4 inhibitors. *Bioorganic & medicinal chemistry letters*, *23*(11), 3325-3328.

17. Ganguli, S. U. B. A. R. N. A., Panigrahi, M. K., Singh, P. R. A. T. I. K. S. H. A., & Shukla, P. K. (2012). One-pot synthesis of novel quinazoline derivatives and their antimicrobial activity. *Int J Pharm Pharm. Sci*, *4*(4), 434-440.

18. Ghorab M. M., Ragab F. A., Alqasoumi S. I., Alafeefy A. M., Aboulmagd S. A., *European journal of medicinal chemistry*. **2010**, *45*(1), 171-178.

19. Lipinski, C. A., Lombardo, F., Dominy, B. W., & Feeney, P. J. (1997). Experimental and computational approaches to estimate solubility and permeability in drug discovery and development settings. *Advanced drug delivery reviews*, *23*(1-3), 3-25.

20. Molinspiration Cheminformatics. Available online: http://www.molinspiration.com/services/properties.html (accessed on 24 March 2019).

21. Jarrahpour, A., Fathi, J., Mimouni, M., Hadda, T. B., Sheikh, J., Chohan, Z., & Parvez, A. (2012). Petra, Osiris and Molinspiration (POM) together as a successful support in drug design: antibacterial activity and biopharmaceutical characterization of some azo Schiff bases. *Medicinal Chemistry Research*, *21*(8), 1984-1990.